JFM RAPIDS
journals.cambridge.org/rapids

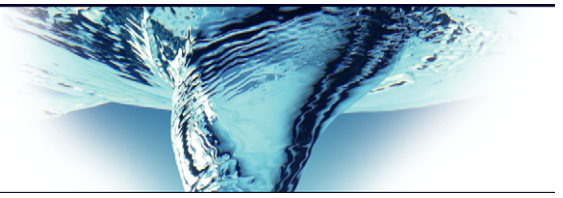

On the logarithmic region in wall turbulence

Ivan Marusic[1],†, Jason P. Monty[1], Marcus Hultmark[2] and Alexander J. Smits[2]

[1]Department of Mechanical Engineering, University of Melbourne, Melbourne, Victoria 3010, Australia
[2]Department of Mechanical and Aerospace Engineering, Princeton University, Princeton, NJ 08544, USA

(Received 16 August 2012; revised 8 October 2012; accepted 11 October 2012)

Considerable discussion over the past few years has been devoted to the question of whether the logarithmic region in wall turbulence is indeed universal. Here, we analyse recent experimental data in the Reynolds number range of nominally $2 \times 10^4 < Re_\tau < 6 \times 10^5$ for boundary layers, pipe flow and the atmospheric surface layer, and show that, within experimental uncertainty, the data support the existence of a universal logarithmic region. The results support the theory of Townsend (*The Structure of Turbulent Shear Flow*, Vol. 2, 1976) where, in the interior part of the inertial region, both the mean velocities and streamwise turbulence intensities follow logarithmic functions of distance from the wall.

Key words: pipe flow boundary layer, turbulent flows, turbulent boundary layers

1. Introduction

A focus area for many decades in the study of wall-bounded turbulence has been the region of the boundary layer known as the inertial sublayer or logarithmic region. The term 'logarithmic' derives from the classical description (see Coles & Hirst 1969), where the mean velocity, U, follows a logarithmic profile with distance from the wall, z:

$$U^+ = \frac{1}{\kappa}\log(z^+) + A. \tag{1.1}$$

Here, $U^+ = U/U_\tau$, where U_τ is the friction velocity, $z^+ = zU_\tau/\nu$, where ν is the kinematic viscosity, κ is the von Kármán constant, and A is a parameter that depends on the roughness of the surface, and is assumed to be a constant for smooth-walled flows. A number of approaches have been used to arrive at (1.1), going back to Prandtl (1925), Kármán (1930) and Millikan (1938), and through to Rotta (1962) and Townsend (1976). While the theoretical arguments may differ, a central feature is that the logarithmic region is associated with a constant velocity scale (U_τ), and any

† Email address for correspondence: imarusic@unimelb.edu.au

doi:10.1017/jfm.2012.511

characteristic lengths scale with z, the distance from the wall. Consistent with this inertial range description, Townsend (1976) proposed that the scaling from the wall can be associated with corresponding attached eddies, whose geometric lengths scale with z, and with population densities per characteristic eddy height that scale inversely with z. Townsend showed that this argument also leads to a logarithmic profile for the streamwise (and spanwise) turbulence intensities of the form

$$\overline{u^2}^+ = B_1 - A_1 \log(z/\delta), \tag{1.2}$$

where $\overline{u^2}^+ = \overline{u^2}/U_\tau^2$ and δ is the boundary-layer thickness (or pipe radius, or channel half-height). Perry & Chong (1982) show mechanistically how (1.1) and (1.2) apply simultaneously in the context of Townsend's attached-eddy hypothesis.

One of the difficulties when discussing the logarithmic region is that the mean velocity profiles deviate very slowly from (1.1), making it difficult to discern where the logarithmic region starts and ends, especially at low Reynolds numbers. This is where it is advantageous to consider more than just the mean velocity profile. Here, we consider (1.1) and (1.2) and require that they both need to apply as the leading-order function for the inertial sublayer to exist. While it has been many years since Townsend proposed (1.2), it is only recently that data have been available at very high Reynolds numbers in order to test the hypothesis properly. Perry and coworkers (Perry & Abell 1977; Perry, Henbest & Chong 1986; Perry & Li 1990; Perry & Marusic 1995) reported an extensive series of experiments towards this goal, but it was clear that their data were not at a sufficiently high Reynolds number to establish unambiguously a logarithmic profile for $\overline{u^2}^+$. Tentative support has also come from other studies, notably Jiménez & Hoyas (2008).

The past decade or so has also seen vigorous discussion challenging the universality of κ, and this topic has been extensively reviewed by Klewicki (2010), Marusic *et al.* (2010), Smits, McKeon & Marusic (2011) and Jiménez (2012). To date, the empirical evidence used to determine κ has come mainly from low to moderately high Reynolds numbers, and, from these, Monkewitz, Chauhan & Nagib (2007, 2008) and Nagib & Chauhan (2008) arrive at $\kappa = 0.384$ for zero-pressure-gradient boundary-layer flows. Monty (2005) obtained similar estimates for κ from studies in pipes and channels for friction Reynolds numbers, $Re_\tau = \delta U_\tau/\nu$, in the range 1000–4000. Studies in the atmosphere by Andreas *et al.* (2006) conclude that $\kappa = 0.387$, which agrees with Nagib & Chauhan (2008) within experimental uncertainty. Very high-Reynolds-number studies in the Princeton Superpipe by McKeon *et al.* (2004) using Pitot tubes have proposed that $\kappa = 0.421$. In the following analysis we use the more recent well-resolved hot-wire measurements of Hultmark *et al.* (2012) to be consistent with the turbulence measurements made in the same study. Owing to the small size of the sensors used in the study by Hultmark *et al.* in combination with the high Reynolds numbers, an extensive logarithmic region was shown also in the streamwise turbulence fluctuations. For more discussions regarding the logarithmic region shown in this dataset, see Hultmark (2012).

In the following we further analyse the recent data from the Superpipe and consider three other recent wall-turbulence datasets at very high Reynolds numbers to test the universality of (1.1) and (1.2).

2. High-Reynolds-number experiments

Four experimental datasets are considered, as summarized in table 1. The first dataset is from the large Melbourne wind tunnel (HRNBLWT; Nickels *et al.* 2005),

Facility	Reference	Re_τ	δ (m)	U_τ (m s^{-1})	ν (m^2 s^{-1})
Melbourne	Kulandaivelu (2012)	18 010	0.3090	0.9362	1.606×10^{-5}
LCC	Winkel *et al.* (2012)	68 780	0.1135	0.5884	9.710×10^{-7}
Superpipe	Hultmark *et al.* (2012)	98 190	0.0647	0.3476	2.290×10^{-7}
SLTEST	Hutchins *et al.* (2012)	$\approx$628 000	$\approx$60	0.1884	1.800×10^{-5}

TABLE 1. Summary of experiments.

which, with a 27 m long working section, was purpose-built for the study of boundary layers that develop over long distances under high-quality flow conditions. The measurements are presented in Kulandaivelu (2012) and are very similar to the results reported by Hutchins *et al.* (2009). A conventional hot wire of 2.5 μm diameter, with a normalized sensing length of $l^+ = 28$, was used with an in-house constant-temperature anemometer (MUCTA). The second dataset is from the study by Winkel *et al.* (2012) conducted in the US Navy's William B. Morgan Large Cavitation Channel (LCC) using laser-Doppler velocimetry. The Princeton Superpipe data are from Hultmark *et al.* (2012), who presented the first documented micro-hot-wire measurements (using NSTAP – Nano-Scale Thermal Anemometry Probe; Bailey *et al.* (2010) and Vallikivi *et al.* (2011)) with a normalized sensing length of $l^+ = 46$ for the Reynolds number presented here. Hutchins *et al.* (2009) discuss the importance of adequate spatial resolution for the turbulence intensity measurements, but it is emphasized that the measurements reported here are adequately resolved for the wall-normal positions considered in this study. This was confirmed by using the correction method proposed by Smits *et al.* (2011) for the effects of limited spatial resolution. As this resulted in only slight changes that do not influence the discussion or conclusions given here, the results are presented with no corrections applied. For completeness, the final dataset considered is from Hutchins *et al.* (2012) for measurements at the SLTEST site in Utah's Western Desert (see also Marusic & Hutchins 2008). They used a wall-normal array of nine sonic anemometers under nominally neutrally buoyant conditions. The spatial resolution of the sonic anemometers, as shown by Kunkel & Marusic (2006) with comparisons to hot wires, is adequate to resolve the measured turbulence intensities in the logarithmic region considered here. Full details of all the measurements are given in the corresponding references.

For each dataset, estimates of the friction velocity U_τ and boundary-layer thickness δ are required. For consistency, the boundary-layer thickness δ was estimated for the Melbourne and LCC results by using a composite law of the wall/wake curve fit using the method of Monkewitz *et al.* (2007), and the same composite profile was used to obtain U_τ for the LCC results using $\kappa = 0.384$ and $A = 4.17$. For the Melbourne results U_τ was estimated using an empirical relation for the skin-friction coefficient

$$\sqrt{2/C_f} = 2.632 \log(Re_{\delta^*}) + 3, \tag{2.1}$$

where $C_f = 2\,(U_\tau/U_\infty)^2$ and Re_{δ^*} is the Reynolds number based on displacement thickness δ^* and free stream velocity U_∞. This estimate for C_f was obtained from a series of measurements of mean wall-shear stress using oil-film interferometry as described in Ng *et al.* (2007) and Chauhan, Ng & Marusic (2010). For the Superpipe measurement, U_τ is determined from the pressure drop in the pipe in the fully developed region, and $\delta = R$, the pipe radius. For the SLTEST measurements U_τ is estimated (in the usual manner for atmosphere surface layer measurements) from

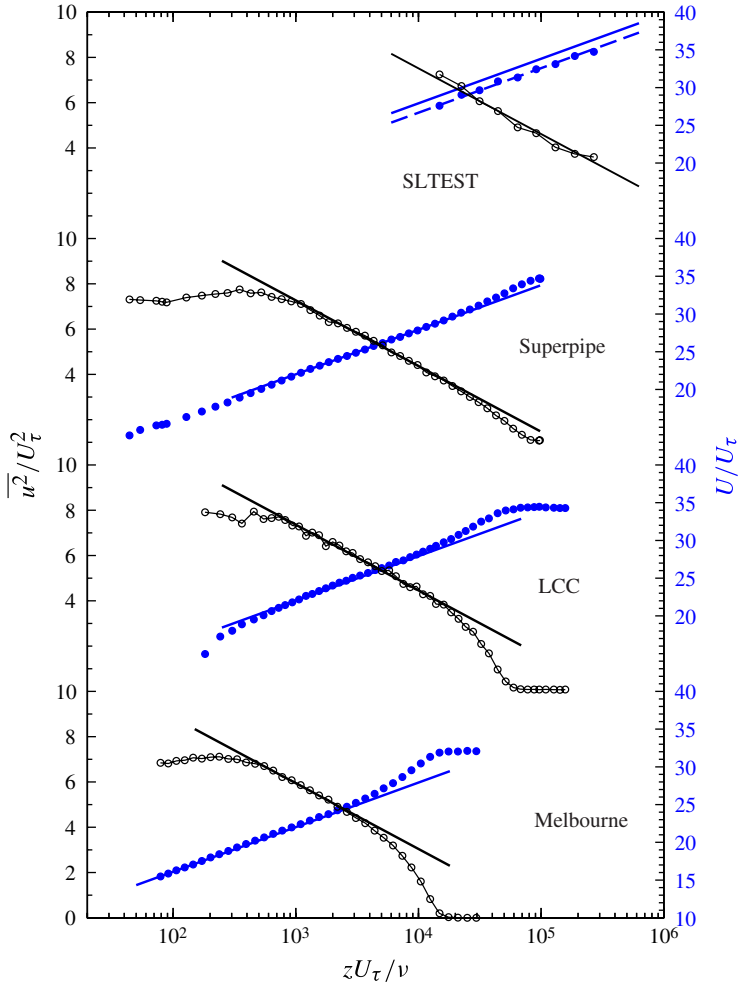

FIGURE 1. Streamwise turbulence intensity and mean velocity profiles: Melbourne wind tunnel, $Re_\tau = 18\,010$ (2.5 μm hot wire); LCC, $Re_\tau = 68\,780$ (LDV); Princeton Superpipe, $Re_\tau = 98\,190$ (NSTAP); SLTEST, $Re_\tau \approx 628\,000$ (Sonics). The solid straight lines correspond to (1.1) and (1.2) with $\kappa = 0.39$, $A = 4.3$ and $A_1 = 1.26$, respectively.

the average value of the Reynolds shear stress ($U_\tau^2 = -\overline{uw}$) across the sonics, as described in Hutchins *et al.* (2012), and the value of δ is roughly estimated based on prior radiosonde measurements that determine the edge of the logarithmic region (see Metzger, McKeon & Holmes 2007).

3. Results and discussion

A compilation of the results is shown in figure 1, and clear support for logarithmic regions is seen for both the mean flow and turbulence intensities. As mentioned earlier, it is difficult to discern the precise locations where the mean velocity profiles deviate from the logarithmic law. However, as seen in figure 1, the turbulence intensity

profiles tend to depart from the logarithmic profile more abruptly than for the mean flow (Marusic & Kunkel 2003; Smits *et al.* 2011). For the mean flow, there are a variety of estimates for the bounds of the logarithmic region. Most studies, including the classical theory, suggest that the outer bound is a fixed fraction of the boundary layer thickness, with typical estimates ranging from 0.1δ to 0.2δ. Accordingly, for our purposes here, we will adopt the outer bound at the location $z/\delta = 0.15$. For the lower bound of the logarithmic region, estimates vary significantly. For example, Tennekes & Lumley (1972) indicate the start of the logarithmic region to be $z^+ > 30$, while Nagib, Chauhan & Monkewitz (2007) suggest $z^+ > 200$, and Zagarola & Smits (1998) adopt $z^+ > 600$ for pipe flows. Recent studies have also questioned the classical theory assumption that the inertial subrange begins at a fixed value of z^+. Zagarola & Smits (1998) showed that the full extent of the viscous influence can exceed $z^+ = 1000$ for the mean velocity at their highest Reynolds numbers in the Superpipe, and studies such as that of Wei *et al.* (2005) have considered the balance of terms in the mean momentum equation to show that viscous effects are expected to extend to z^+ values that scale with $Re_\tau^{1/2}$. In line with this, Eyink (2008) demonstrated the possibility of incorporating a $Re_\tau^{1/2}$ dependence to a modified attached-eddy approach to account for near-wall viscous effects, and Klewicki, Fife & Wei (2009) estimated that the mean viscous force loses leading-order influence for $z^+ \geqslant 2.6Re_\tau^{1/2}$ in all turbulent wall flows.

In this paper we are focused on testing the universality of (1.1) and (1.2) at sufficiently high Reynolds numbers, and for the purpose of curve fitting the parameters in these equations we choose an estimate for the lower bound of the logarithmic region to be $z^+ = 3Re_\tau^{1/2}$. We consider this estimate to be conservative, as all the above studies would agree that the present data in the range $3Re_\tau^{1/2} < z^+ < 0.15Re_\tau$ fall within the logarithmic region, and thus we are effectively weighting the data points in the logarithmic region in which we have most confidence. It is noted, however, that using this range gives good agreement with the logarithmic regions for the streamwise turbulence intensities as highlighted in figure 2. Figure 3 indicates how the $3Re_\tau^{1/2} < z^+ < 0.15Re_\tau$ logarithmic range corresponds for the laboratory mean flows, where here the differences from the logarithmic profile are emphasized by subtracting a logarithmic function with $\kappa = 0.39$. The difficulties in estimating the departure locations are exacerbated by the slow and weak deviations at levels of the order of the measurement uncertainty. Overall, the results in figure 3 show trends that are reasonably consistent with the chosen logarithmic region bounds. For completeness, we also show in figure 4 that the $3Re_\tau^{1/2}$ bound corresponds reasonably well for the Superpipe data of Hultmark *et al.* (2012) at other Reynolds numbers. At the lower Reynolds numbers, no clear logarithmic region in the mean flow nor the turbulence intensities exists. It is worth noting that using the bounds $3Re_\tau^{1/2} < z^+ < 0.15Re_\tau$ for one decade of a logarithmic region requires the friction Reynolds number to exceed $Re_\tau > 40\,000$, and thus it is essential to have very high-Reynolds-number data as is the case here.

It is emphasized that figures 2–4 do not prove that the adopted bounds are correct (for this, further work and data at higher Reynolds numbers are needed) but they do confirm that this range can be used as a reasonable estimate for the extent of the logarithmic region.

3.1. *Compatibility with attached-eddy model*

Adopting a Reynolds-number-dependent lower bound of the logarithmic region in wall units conflicts with most classical theories, but it should not be regarded as

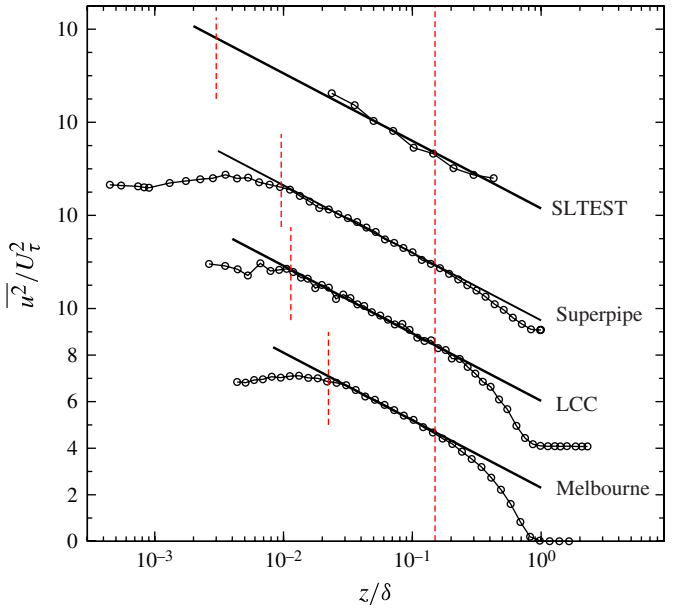

FIGURE 2. Turbulence intensity profiles. The solid lines have slope with $A_1 = 1.26$. The dashed vertical lines indicate the region $3Re_\tau^{1/2} < z^+ < 0.15Re_\tau$.

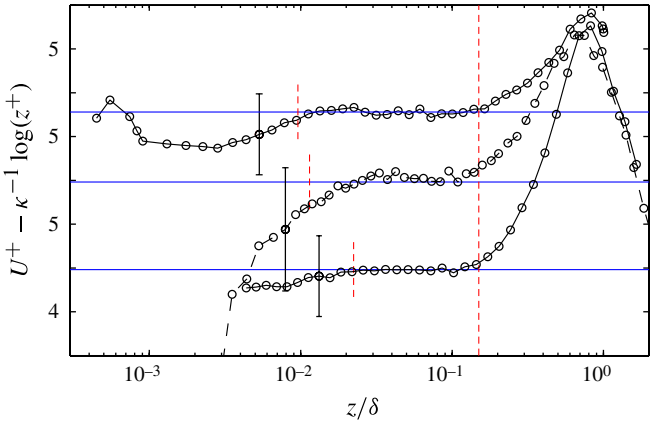

FIGURE 3. Mean velocity profiles with log law function, where $\kappa = 0.39$, subtracted for the Superpipe, LCC and Melbourne datasets (shown in order from top to bottom). The dashed vertical lines indicate the region $3Re_\tau^{1/2} < z^+ < 0.15Re_\tau$, and the horizontal lines indicate the best fit for this range highlighting the log region plateau. Error bars of U^+ are shown at the indicated locations.

incompatible with Townsend's theory. In fact, Townsend (1976) does not specify the bounds and simply states that, for (1.2) to hold, $l_0 \ll z \ll \delta$, where l_0 scales with the size of the smallest attached eddy. This implies that the Reynolds number must

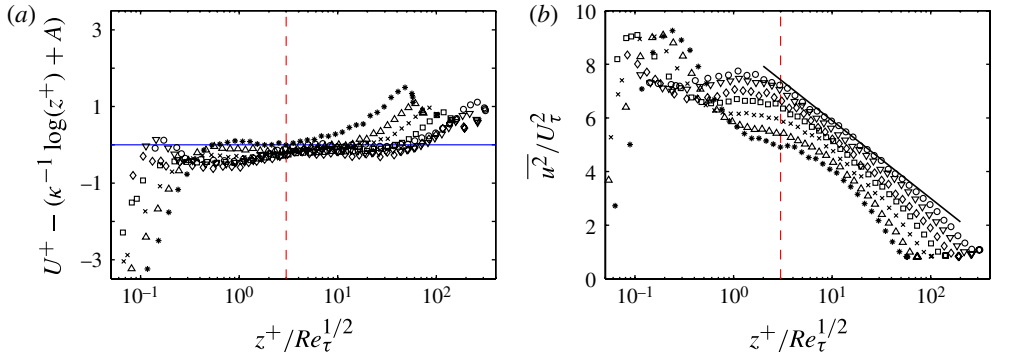

FIGURE 4. Superpipe data of Hultmark *et al.* (2012) shown versus $z^+/Re_\tau^{1/2}$ for $Re_\tau =$ 3330, 5410, 10 480, 20 250, 37 450, 68 370, 98 190. Dashed vertical line indicates $z^+ = 3Re_\tau^{1/2}$. The mean flow deviation is with $\kappa = 0.39$, $A = 4.3$, and the solid black line is (1.2) for the highest Reynolds-number case with $A_1 = 1.26$, $B_1 = 1.56$.

be sufficiently high, and asymptotically the condition holds for $l_0^+ \sim Re_\tau^n$, provided $n < 1$. Perry & Marusic (1995) showed that Reynolds-number effects could possibly be accounted for in the attached-eddy model by limiting the range of scales of attached eddies. This leads to a peak in the Reynolds shear stress (see figure 5 of Perry & Marusic 1995). A similar attached-eddy cut-off was also used by Marusic, Uddin & Perry (1997) in their formulation for $\overline{u^2}^+$ to account for departures from (1.2), but there it was assumed that $l_0^+ = 100$. This would lead to the peak in Reynolds shear stress also being located at $l_0^+ = O(100)$. However, extensive evidence now exists, both empirical (Sreenivasan & Sahay 1997) and from theory (Klewicki *et al.* 2009), that the peak Reynolds shear stress occurs at a z^+ location that scales with $Re_\tau^{1/2}$, and for the attached-eddy model to reproduce this result requires $l_0^+ \sim Re_\tau^{1/2}$. The attached-eddy model kinematically accounts for the entire field, and the mean flow and turbulence cannot be regarded separately. Therefore, if $l_0^+ \sim Re_\tau^{1/2}$ is adopted, then the attached-eddy model leads to a $z^+ \sim Re_\tau^{1/2}$ lower bound for all components of the Reynolds stress and the mean flow.

3.2. *Estimates of constants and note of caution*

Using the experimental datasets for each facility in the range $3Re_\tau^{1/2} < z^+ < 0.15Re_\tau$, estimates of the constants and coefficients in (1.1) and (1.2) were found using least-squares error curve fits, and the results are summarized in table 2. It is clear that results from the three laboratory facilities show remarkably similar log law constants, and the atmospheric case is consistent with these within experimental error. An analysis of all the datasets together (weighted on experimental uncertainty for measurement set and the respective number of points in the logarithmic region) leads to estimates of the von Kármán constant $\kappa = 0.39$ with $A = 4.3$, and of the Townsend–Perry constant $A_1 = 1.26$. The solid lines drawn in figure 1 are log laws with these constants, and excellent agreement with universal (1.1) and (1.2) is seen. It is noted that the SLTEST data are for a mildly transitional rough surface, and therefore for universality we expect κ to be the same but A to vary. This point is highlighted in figure 1 with the dashed straight line, which also has $\kappa = 0.39$, but with a lower

Facility	A_1	B_1	κ	A
LCC	1.21 ± 0.08	2.20 ± 0.25	0.384^*	4.17^*
Melbourne	1.26 ± 0.06	2.30 ± 0.18	0.387 ± 0.004	4.32 ± 0.20
Superpipe	1.23 ± 0.05	1.56 ± 0.16	0.391 ± 0.004	4.34 ± 0.19
SLTEST	1.33 ± 0.17	2.14 ± 0.40	0.410 ± 0.028	4.44 ± 1.83

TABLE 2. Parameters in (1.1) and (1.2) obtained from least-squares error curve fit for data in the region $3Re_\tau^{1/2} < z^+ < 0.15Re_\tau$. The uncertainty estimates are based on 95 % confidence bounds from the curve-fitting procedure. An asterisk denotes values where a composite formulation was used to determine U_τ with these assumed constants.

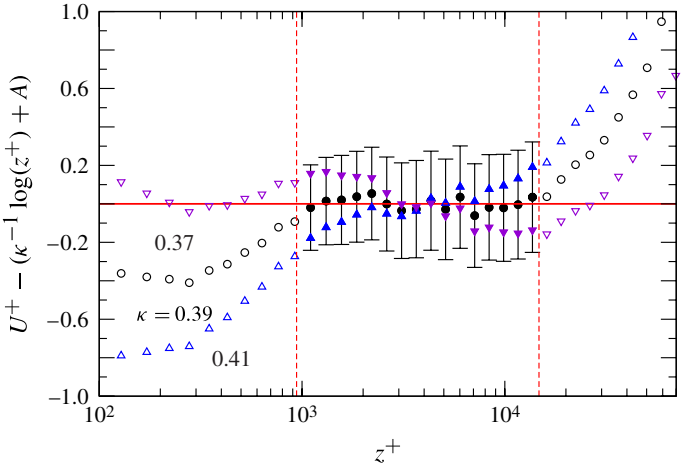

FIGURE 5. Mean velocity profile with log law subtracted for Superpipe data. Error bars shown correspond to ± 1 % uncertainty in U^+. The additive constant in the logarithmic law, A, is calculated so as to minimize the root-mean-square error in the region in between the vertical lines, corresponding to $3Re_\tau^{1/2} < z^+ < 0.15Re_\tau$. Here, $\kappa = 0.37,\ A = 3.13$, $\kappa = 0.39,\ A = 4.28$, and $\kappa = 0.41,\ A = 5.31$.

value of A ($A = 3.1$). This result is consistent with the estimated sand grain roughness height of $k_s^+ \approx 21$ in the SLTEST experiments (Hutchins *et al.* 2012). It is also noted that B_1 in (1.2) is not expected to be constant between these different wall-bounded flows. As discussed by Marusic & Perry (1995), B_1 will depend on the wake parameter and flow geometry and therefore is expected to be different between pipes and zero-pressure-gradient (ZPG) boundary layers. It is also noted that the LCC dataset has a weak favourable pressure gradient, and therefore will have a smaller wake component than a precise ZPG flow. It should be noted that, while values of $\kappa = 0.39$ and $A_1 = 1.26$ are seen to fit the data well, there remains considerable uncertainty as to the precise values of these constants with the present limited datasets. The uncertainties for κ are highlighted in figure 5 for the Superpipe mean velocity data. The error bars shown in the figure are considered conservative, as they correspond to ± 1 % uncertainty in U/U_τ. The figure shows that, within the considered logarithmic region (indicated by the vertical dashed lines), the differences between $\kappa = 0.39 \pm 0.02$ cannot

be discerned beyond the error bars. The value of $\kappa = 0.421$ reported by McKeon *et al.* (2004) in the Superpipe probably exceeds these bounds, and the possible reasons for differences between Pitot tube and hot-wire mean-velocity measurements are the subject of ongoing study. The uncertainties for the boundary-layer datasets are likely to be greater because of the additional uncertainties in U_τ, given that no direct measurements of the wall-shear stress were made in these experiments. Overall, it is emphasized that this paper is not meant to be definitive in determining the value of κ (nor the bounds of the logarithmic region). Rather, it indicates that these four high-Reynolds-number flows exhibit logarithmic behaviour that is consistent with a universal von Kármán constant, and this differs from the view that has emerged over the past decade or so.

4. Conclusions

Recent experimental studies in the Reynolds-number range of nominally $2 \times 10^4 < Re_\tau < 6 \times 10^5$ for boundary layers, pipe flow and the atmospheric surface layer support the existence of a universal logarithmic region. The results support the theory of Townsend (1976) and Perry & Chong (1982) that the interior part of the inertial region requires both a logarithmic profile for the mean flow and the streamwise turbulence intensities. Within the experimental uncertainties, all the data are well described with a nominal von Kármán constant $\kappa = 0.39$, and a Townsend–Perry constant $A_1 = 1.26$. The experimental data are unique given the high Reynolds numbers presented and the fidelity of the measurement techniques, where both the mean velocity and the streamwise turbulence intensities are measured with the same instrument.

Acknowledgements

The authors wish to thank the Australian Research Council, ONR under Grant N00014-09-1-0263 (Program Manager R. Joslin), and NSF under Grant CBET-1064257 (Program Manager H. Winter) for the financial support of this research. We also gratefully acknowledge the anonymous reviewers for helpful comments, and Professor D. Dowling for kindly making available the LCC data.

References

ANDREAS, E. L., CLAFFEY, K. J., JORDAN, R. E., FAIRALL, C. W., GUEST, P. S., PERSSON, P. O. G. & GRACHEV, A. A. 2006 Evaluations of the von Kármán constant in the atmospheric surface layer. *J. Fluid Mech.* **559**, 117–149.

BAILEY, S.C.C., KUNKEL, G.J., HULTMARK, M., VALLIKIVI, M., HILL, J.P., MEYER, K.A., TSAY, C., ARNOLD, C.B. & SMITS, A.J. 2010 Turbulence measurements using a nanoscale thermal anemometry probe. *J. Fluid Mech.* **663**, 160–179.

CHAUHAN, K., NG, H. C. H. & MARUSIC, I. 2010 Empirical mode decomposition and Hilbert transforms for analysis of oil-film interferograms. *Meas. Sci. Tech.* **21**, 105405, 1–13.

COLES, D. E. & HIRST, E. A. 1969 Compiled data. In *Proceedings of Computation of Turbulent Boundary Layers, AFOSR-IFP Stanford Conference 1968*, Vol.II.

EYINK, G. L. 2008 Turbulent flow in pipes and channels as cross-stream 'inverse cascades' of vorticity. *Phys. Fluids* **20**, 125101.

HULTMARK, M. 2012 A theory for the streamwise turbulent fluctuations in high Reynolds number pipe flow. *J. Fluid Mech.* **707**, 575–584.

HULTMARK, M., VALLIKIVI, M., BAILEY, S. C. C. & SMITS, A. J. 2012 Turbulent pipe flow at extreme Reynolds numbers. *Phys. Rev. Lett.* **108**, 094501.

HUTCHINS, N., CHAUHAN, K., MARUSIC, I., MONTY, J. P. & KLEWICKI, J. 2012 Towards reconciling the large-scale structure of turbulent boundary layers in the atmosphere and laboratory. *Boundary-Layer Meteorol.* **145** (2), 273–306.

HUTCHINS, N., NICKELS, T. B., MARUSIC, I. & CHONG, M. S. 2009 Hot-wire spatial resolution issues in wall-bounded turbulence. *J. Fluid Mech.* **635**, 103–136.

JIMÉNEZ, J. 2012 Cascades in wall-bounded turbulence. *Annu. Rev. Fluid Mech.* **44**, 27–45.

JIMÉNEZ, J. & HOYAS, S. 2008 Turbulent fluctuations above the buffer layer of wall-bounded flows. *J. Fluid Mech.* **611**, 215–236.

VON KÁRMÁN, T. 1930 Mechanische ähnlichkeit und turbulenz. *Gött. Nachr.* 58–76.

KLEWICKI, J. C. 2010 Reynolds number dependence, scaling, and dynamics of turbulent boundary layers. *Trans. ASME J. Fluids Engng* **132**, 094001.

KLEWICKI, J. C., FIFE, P. & WEI, T. 2009 On the logarithmic mean profile. *J. Fluid Mech.* **638**, 73–93.

KULANDAIVELU, V. 2012 Evolution of zero pressure gradient turbulent boundary layers from different initial conditions. PhD thesis, University of Melbourne.

KUNKEL, G. J. & MARUSIC, I. 2006 Study of the near-wall-turbulent region of the high-Reynolds-number boundary layer using an atmospheric flow. *J. Fluid Mech.* **548**, 375–402.

MARUSIC, I. & HUTCHINS, N. 2008 Study of the log-layer structure in wall turbulence over a very large range of Reynolds number. *Flow Turbul. Combust.* **81**, 115–130.

MARUSIC, I. & KUNKEL, G. J. 2003 Streamwise turbulence intensity formulation for flat-plate boundary layers. *Phys. Fluids* **15**, 2461–2464.

MARUSIC, I., MCKEON, B. J., MONKEWITZ, P., NAGIB, H. M., SMITS, A. J. & SREENIVASAN, K. R. 2010 Wall-bounded turbulent flows: recent advances and key issues. *Phys. Fluids* **22**, 065103.

MARUSIC, I. & PERRY, A. E. 1995 A wall wake model for the turbulent structure of boundary layers. Part 2. Further experimental support. *J. Fluid Mech.* **298**, 389–407.

MARUSIC, I., UDDIN, M. & PERRY, A. E 1997 Similarity law for the streamwise turbulence intensity in zero-pressure-gradient turbulent boundary layers. *Phys. Fluids* **12**, 3718–3726.

METZGER, M., MCKEON, B. J. & HOLMES, H. 2007 The near-neutral atmospheric surface layer: turbulence and non-stationarity. *Phil. Trans. R. Soc. Lond.* A **365**, 859–876.

MCKEON, B. J., LI, J., JIANG, W., MORRISON, J. & SMITS, A. J. 2004 Further observations on the mean velocity distribution in fully developed pipe flow. *J. Fluid Mech.* **501**, 135–147.

MILLIKAN, C. M. 1938 A critical discussion of turbulent flows in channels and circular tubes. In *Proceedings of the Fifth International Congress for Applied Mechanics, Harvard and MIT, 12–26 September*. Wiley.

MONKEWITZ, P. A., CHAUHAN, K. A. & NAGIB, H. M. 2007 Self-contained high-Reynolds-number asymptotics for zero-pressure-gradient turbulent boundary layers. *Phys. Fluids* **19**, 115101.

MONKEWITZ, P. A., CHAUHAN, K. A. & NAGIB, H. M. 2008 Comparison of mean flow similarity laws in zero pressure gradient turbulent boundary layers. *Phys. Fluids* **20**, 105102.

MONTY, J. P. 2005 Developments in smooth wall turbulent duct flows. PhD thesis, University of Melbourne.

NAGIB, H. M. & CHAUHAN, K. A. 2008 Variations of von Kármán coefficient in canonical flows. *Phys. Fluids* **20**, 101518.

NAGIB, H. M., CHAUHAN, K. A. & MONKEWITZ, P. A. 2007 Approach to an asymptotic state for zero pressure gradient turbulent boundary layers. *Phil. Trans. R. Soc. Lond.* A **365**, 755.

NG, H. C. H., MARUSIC, I., MONTY, J. P., HUTCHINS, N. & CHONG, M. S. 2007 Oil-film interferometry in high Reynolds number turbulent boundary layers. In *Proceedings of the 16th Australasian Fluid Mechanics Conference, Gold Coast, Australia*.

NICKELS, T. B., MARUSIC, I., HAFEZ, S. M. & CHONG, M. S. 2005 Evidence of the k^{-1} law in a high-Reynolds-number turbulent boundary layer. *Phys. Rev. Lett.* **95**, 074501.

PERRY, A. E. & ABELL, C. J. 1977 Asymptotic similarity of turbulence structures in smooth- and rough-walled pipes. *J. Fluid Mech.* **79**, 785–799.

PERRY, A. E. & CHONG, M. S. 1982 On the mechanism of wall turbulence. *J. Fluid Mech.* **119**, 173–217.

PERRY, A. E., HENBEST, S. M. & CHONG, M. S. 1986 A theoretical and experimental study of wall turbulence. *J. Fluid Mech.* **165**, 163–199.

PERRY, A. E. & LI, J. D. 1990 Experimental support for the attached eddy hypothesis in zero pressure-gradient turbulent boundary layers. *J. Fluid Mech.* **218**, 405–438.

PERRY, A. E. & MARUSIC, I. 1995 A wall-wake model for the turbulence structure of boundary layers. Part 1. Extension of the attached eddy hypothesis. *J. Fluid Mech.* **298**, 361–388.

PRANDTL, L. 1925 Bericht über untersuchungen zur ausgebildeten turbulenz. *Z. Angew. Math. Mech.* **5**, 136–139.

ROTTA, J. C. 1962 Turbulent boundary layers in incompressible flow. *Prog. Aerosp. Sci.* **2**, 1–219.

SMITS, A. J., MCKEON, B. J. & MARUSIC, I. 2011 High Reynolds number wall turbulence. *Annu. Rev. Fluid Mech.* **43**, 353–375.

SMITS, A. J., MONTY, J. P., HULTMARK, M., BAILEY, S. C. C., HUTCHINS, N. & MARUSIC, I. 2011 Spatial resolution correction for wall-bounded turbulence measurements. *J. Fluid Mech.* **676**, 41–53.

SREENIVASAN, K. R. & SAHAY, A. 1997 The persistence of viscous effects in the overlap region and the mean velocity in turbulent pipe and channel flows. In *Self-Sustaining Mechanisms of Wall Turbulence* (ed. R. Panton). pp. 253–272. Computational Mechanics Publications.

TENNEKES, H. & LUMLEY, J. L. 1972 *A First Course in Turbulence*. MIT Press.

TOWNSEND, A. A. 1976 *The Structure of Turbulent Shear Flow*, Vol. 2. Cambridge University Press.

VALLIKIVI, M., HULTMARK, M., BAILEY, S. C. C. & SMITS, A. J. 2011 Turbulence measurements using a nanoscale thermal anemometry probe. *Exp. Fluids* **51** (6), 1521–1527.

WEI, T., FIFE, P., KLEWICKI, J. C. & MCMURTRY, P. 2005 Properties of the mean momentum balance in turbulent boundary layer, pipe and channel flows. *J. Fluid Mech.* **522**, 303–327.

WINKEL, E. S., CUTBIRTH, J. M., CECCIO, S. L., PERLIN, M. & DOWLING, D. R. 2012 Turbulence profiles from a smooth flat-plate turbulent boundary layer at high Reynolds number. *Exp. Therm. Fluid Sci.* **40**, 140–149.

ZAGAROLA, M. V. & SMITS, A. J. 1998 Mean-flow scaling of turbulent pipe flow. *J. Fluid Mech.* **373**, 33–79.